Volume 1, Number 1, 24-31, April 2003

International Journal of
Vascular Biomedical Engineering

Red Blood Cell Velocity Field in Rat Mesenteric Arterioles Using Micro PIV Technique

Y Sugii[1¶], S Nishio[2], K Okamoto[1], A Nakano[3], M Minamiyama[3] and H Niimi[3]

1 Nuclear Engineering Research Laboratory, University of Tokyo
2 Department of Maritime Science, Kobe University of Mercantile Marine Fukae-Minami, Higashinada
3 Department of Vascular Physiology, National Cardiovascular Center Research Institute Suita

Abstract

As endothelial cells are subject to flow shear stress, it is important to determine the detailed velocity distribution in microvessels in the study of mechanical interactions between blood and endothelium. This paper describes a velocity field of the arteriole in the rat mesentery using an intravital microscope and high-speed digital video system obtained by a highly accurate PIV technique. Red blood cells (RBCs) velocity distributions with spatial resolutions of 0.8 × 0.8 μm were obtained even near the wall in the center plane of the arteriole. By making ensemble-averaged time-series of velocity distributions, velocity profiles over different cross-sections were calculated for comparison. The shear rate at the vascular wall also evaluated on the basis of the ensemble-averaged profiles. It was shown that the velocity profiles were blunt in the center region of the vessel cross-section while they were steep in the near wall region. The wall shear rates were significantly small, compared with those estimated from the Poiseuille profiles.

Key words: Blood Flow, RBC Velocity, Microcirculation, Biofluid, Micro PIV

Introduction

Blood flow in microvessels (arterioles, capillaries and venules), whose diameter ranges from 5 to 50 μm, is responsible for the maintenance of tissue and organ functions. The accurate measurement of microvascular flow velocity is essential for basic and clinical studies on the assessment of flow shear stress at the vascular wall in relation to substance exchange between blood and tissue.

Since blood is mainly composed of red blood cells (RBCs) and plasma, blood shows multi-phase and non-Newtonian flow natures differently from homogeneous and Newtonian fluids. The blood viscosity is increased markedly at low flow shear-rates due to RBC's aggregation, while it remains almost constant at high flow shear-rates. Blood flow in microvessels shows flow features that RBCs drift to the central axis of vessel (*axial drift*) and that a cell-free layer is formed along the vascular wall (plasma layer)[1].

Various measurement techniques have been developed to investigate blood flow velocity in microvessels, including dual slit (window) method[2-5], laser Doppler velocimetry[6,7], videoimage technique[8-11] and so on. These techniques, however, cannot provide velocity distributions with high spatial resolution and measurement accuracy enough to evaluate the flow shear-rate at the vascular wall. For this reason, the wall shear-rate has been estimated by assuming the Poiseuille profile on the basis of the measured flow-rate[12,13].

Particle image velocimetry (PIV) is a quantitative

¶ Tokai-mura, Ibaraki, 319-1188, Japan
E-mail: sugii@utnl.jp

method for measuring velocity fields instantaneously in experimental fluid mechanics systems[14,15]. A number of PIV methods, such as the cross-correlation method, particle tracking method and iterative correlation method, have been proposed to improve measurement accuracy and spatial resolution in macro flows. The main feature of these methods, measurement accuracy and utility in a range of experimental conditions, has been comprehensively investigated both experimentally and theoretically.

The authors developed a highly accurate PIV technique with improved measurement accuracy and spatial resolution[16,17], and applied the technique to blood flow in rat mesenteric arterioles on basis of high-speed digital videomicroscopic images. By taking the motion of mesentery tissue into account, the accuracy of RBC velocity could be improved greatly[18]. It was demonstrated that in vivo microvascular flows might be influenced greatly by multi-phase and non-Newtonian natures of blood as well as cardiac cycle.

This paper aimed to comprehensively describe in vivo microvascular flow measurement using a micro-PIV technique based on high-speed digital videomicroscopic images. The velocity field of red blood cells (RBCs) in arteriolers of rat mesentery using an intravital microscope and high-speed digital video system was investigated. By making ensemble-averaged time-series of velocity distributions, velocity profiles over different cross-sections were calculated for comparison. The shear rate at the vascular wall evaluated on the basis of the ensemble-averaged profiles and compared with those estimated from the Poiseuille profiles.

Materials and Methods

Blood Flow Image

Figure 1 shows a schematic view of experimental set up. A mesenteric arteriole of a rat was observed using an intravital microscope with a water-immersion objective lens (CFI Fluor 60×W, Nikon, Japan), with magnification M = 60 and numerical aperture NA = 1.0. Male Wister rats (8 weeks, 300 g body weight) were anesthetized with thiobutabarbital

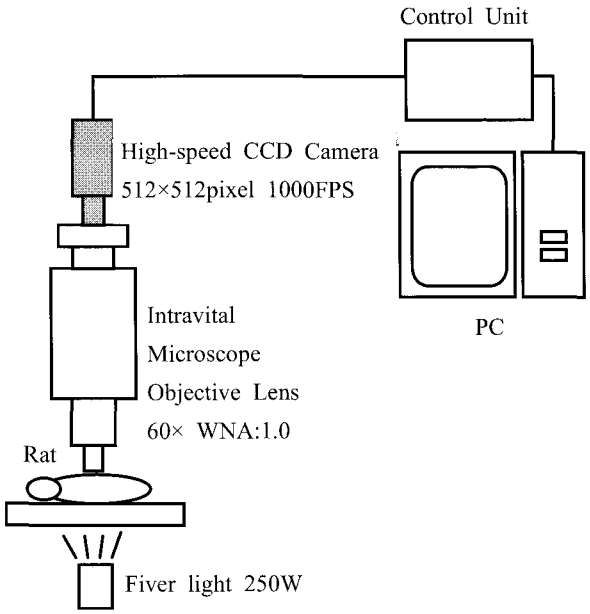

Figure 1 Schematic view of experimental set up for visualization of in vivo blood flow of rat mesenteric arteriole.

sodium intraperitoneously, and allowed to respire spontaneously. An intestinal loop was mounted on the stage of the microscope. The mesentery was placed on an observation window and perfused with Krebs-Ringer solution maintained at 37℃. Blood flow images were recorded into computer for a period of approximately 2 sec (2048 images) using a high-speed CCD camera (Weinberger SpeedCAMpro, Dietikon, Switzerland) at 1000 frames/sec. Images were captured at a resolution of 512 × 512 pixels in 8-bit grayscale. The measurement region was backlit using a 250 W direct-current metal halide lamp. The illumination was filtered through a 546-nm green interference filter in order to enhance the contrast of the RBC (Red Blood Cell) images. The basic flow features were initially investigated by examining a relatively straight length of arteriole. The arterial blood pressure was continuously monitored via a catheter inserted in a carotid artery.

Figure 2 shows a captured image of blood flow in a mesenteric arteriole. The observed region was 136 × 136 μm in size, with each pixel representing a 0.27 × 0.27 μm area. The estimated internal diameter of the vessel was 24 to 26 μm calculated by image analysis technique. The vessel curved slightly to the right at around x = 50 μm. Generally,

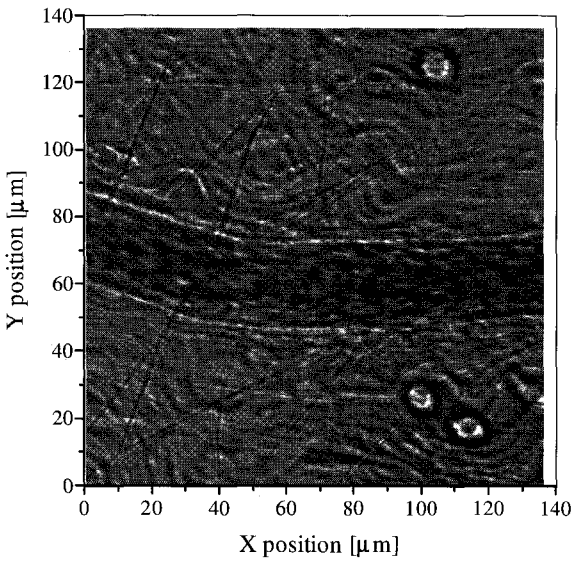

Figure 2 Blood flow image of a rat mesenteric arteriole.

the diameter of endothelial cells is approximately 5 μm. However, the apparent diameter of these cells in the present images is 2 to 4 μm. This may be attributed to the out-of-plane alignment of the cells in the optical plane. A plasma layer, in which very few cells passed, was clearly observed near the wall.

Analysis method

In all of previous studies, RBC velocity vector is obtained by applying the PIV technique to 2 successive images without taking mesentery motion into account. The relative position of the RBC velocity vector to vessel wall always moves with time due to vibration of vessel itself or tissue caused by cardiac beat. Therefore, bias error due to mesentery motion interfered with the analysis of instantaneous RBC velocity.

In order to improve measurement accuracy by taking a mesentery motion into account a new method was proposed[18], in which both the blood image and RBC velocity were modified using a mesentery motion obtained by highly accurate PIV technique. The PIV technique was applied to two successive shifted images. The measurement accuracy of RBC velocity improved after the relative positions of the arteriole in all images were arranged consistently and the effect of the mesentery motions eliminated.

Analyzing the mesentery motion, it was considered the motion involved only parallel translation, without higher-order displacements such as deformation or rotation. The method can improve measurement accuracy.

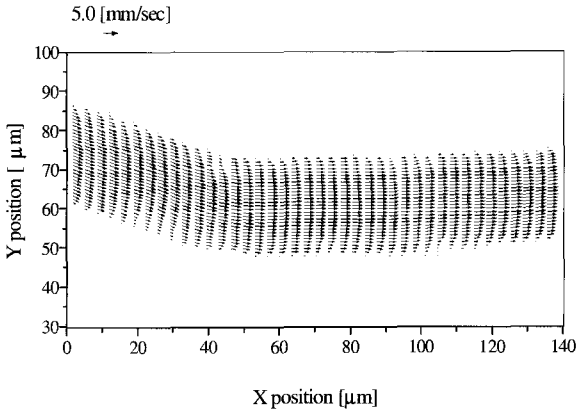

Figure 3 Time-averaged velocity distribution of blood flow in arteriole obtained by PIV technique.

Results

Figure 3 shows the time-averaged velocity distributions of 2048 images for 2 sec of blood flow in an arteriole, calculated using the PIV technique described in the previous section. The obtained RBC velocity distribution consists of 2047 maps at 1000 Hz. An interrogation window of 7 × 7 pixels was taken with 50% overlap, corresponding to a spatial resolution of 0.8 × 0.8 μm. The velocities in the horizontal direction were thinned out for clarity. Since the mesentery motion was taken into account, the obtained velocities in the region outside of the arteriole are zero. The velocity vectors very close to the wall were measured and it was found that the wall-normal components of the velocity vectors were close to zero. Low velocities were also observed at the inside wall of a blunt corner in the arteriole. It is considered that white blood cells were attached to the vessel wall in that area checked by visual observation varying focal plane. Since the interrogation window size was smaller than the size of red blood cells, groups of 3 to 4 similar velocity vectors occurred in some regions. The maximum velocity was about 11.0 pixels/frame or 3.0 mm/s at the center of the arteriole. The velocity vectors on the lower side, at x = 100 to 120 μm in particular, were smaller than the values expected for laminar flow. It is

considered that the RBC velocity was reduced due to the presence of a plasma layer. Analyzing the time series of axial blood velocity in several cross sections on the lower streamside at the bend in the vessel, the velocities showed periodical because of a heartbeat. The amplitudes and phases in all sections were relatively consistent. However, some anomalous peaks were observed due to the inclusion of spurious vectors. The peak frequency was about 6.4 Hz obtained by spectrum analysis. The result shows that the velocity is synchronized with the cardiac cycle of 6-7 Hz even in microvessels.

Since blood density ρ is about 1.05 g/cm^3 and apparent viscosity of blood μ is about 2.5 cP, Reynolds number Re and Womersley parameter α are 3.3-3.4 × 10^{-2} and 4.8-5.3 × 10^{-2} in several cross sections, approximately. Womersley parameter α, which represents the pulse frequency, is defined as,

$$\alpha = R\sqrt{\frac{2\pi\rho f}{\mu}} \tag{1}$$

where f shows cardiac cycle.

Since Reynolds number and Womersley parameter are very small, the flow is regarded as a laminar and quasi-steady flow. Therefore, an ensemble averaging using the results of spectrum analysis was carried out. Figure 4 shows the phase-averaged axial velocity at the center at four cross sections x = 53, 85, 101, 125 μm normalized using cardiac cycle T = 155 msec. These profiles were obtained using 13 cardiac cycles. The velocities in every section repeatedly increased sharply from end diastole at time t/T = 0 toward a peak systole at time t/T = 0.26, and then decreased gradually toward a late diastole. In the region of reducing the speed around at t/T = 0.4 to 0.8, fluctuation was also observed. High cross correlations for these series were recognized. The pulsed flow was similar to that of regular circulatory flow. However, the velocities did not become zero at end diastoles because of inertia forces. This is consistent with the results obtained in previous studies using the dual-slit method, LDV and other methods. The diameters of vessels at x = 53, 85, 101 and 125 m were D = 24.9, 24.7, 25.7 and 23.6 μm, respectively. Time-averaged velocities at these sections were 3.27, 3.15, 3.11 and 3.54 mm/s, respectively. Since the most downstream section at (d) x = 125 μm had the smallest diameter, the velocity was largest varied from 3.0 mm/s to 4.2 mm/s. However, other three velocity profiles for different diameters have almost similar values from 2.6 mm/s to 3.7 mm/s. Very low velocity region observed near the wall might be influenced by the marginal cell-free layer.

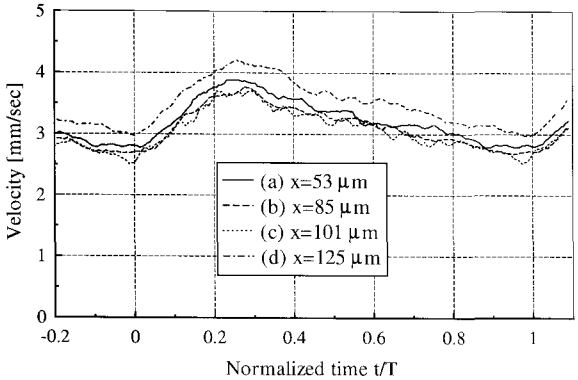

Figure 4 Ensemble-averaged axial velocity over time at the center in four cross sections.

Figure 5 shows the phase-averaged axial blood velocity profiles in four cross-sections shown in Figure 4. These profiles show at four phase t/T=0.0 (end diastole), 0.13 (acceleration), 0.26 (peak systole) and 0.58 (deceleration). Thirty velocity values were obtained along the capillary diameter at a spacing of 0.8 μm. The time averaged velocity profiles in every section are displayed as dot lines. The wall positions and capillary diameter in each section are displayed in the figure. The wall position was identified via the luminance of the cross section in time-averaged image after mesentery motion compensation. The velocity of all profiles became maximal around the center of the vessel, and decreased to zero near the wall. The velocities were zero outside the arteriole because of improving the error caused by mesentery motion. The arteriole velocity profiles were broad at the center of the vessel, and sharp near the wall compared with a parabolic flow profile, and then a gentle velocity gradient near the wall. The profiles in every stage at x = 85 μm in Fig. 5 (b) shows symmetric. However, the profile at 125

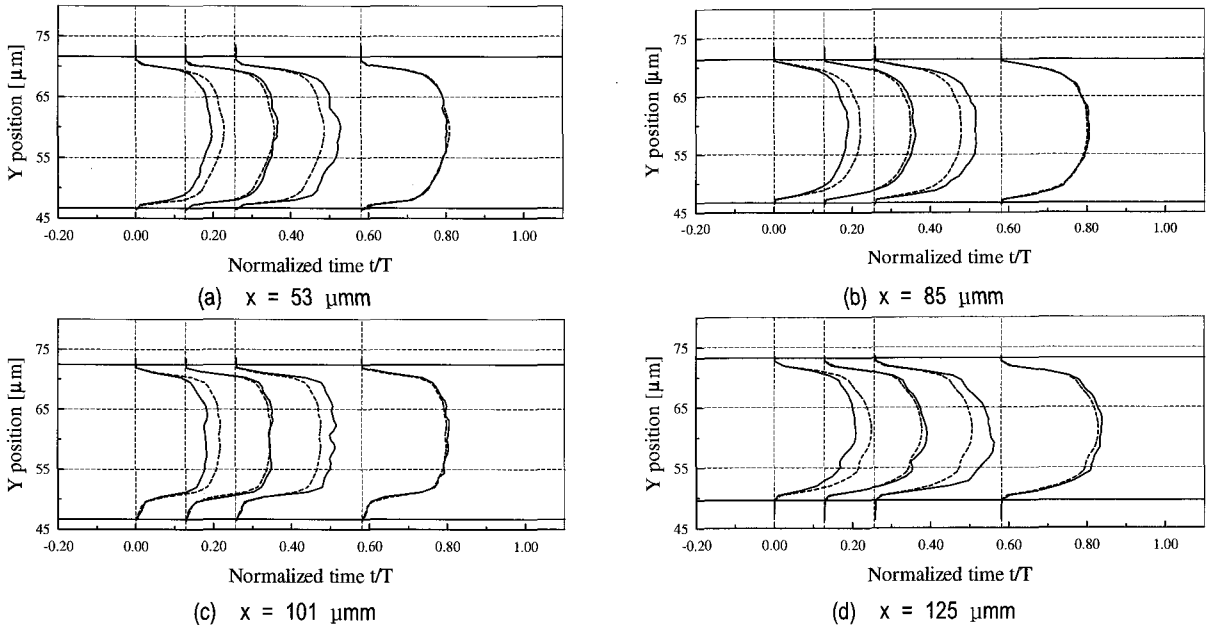

Figure 5 Ensemble-averaged axial velocity profiles over time in four cross sections.

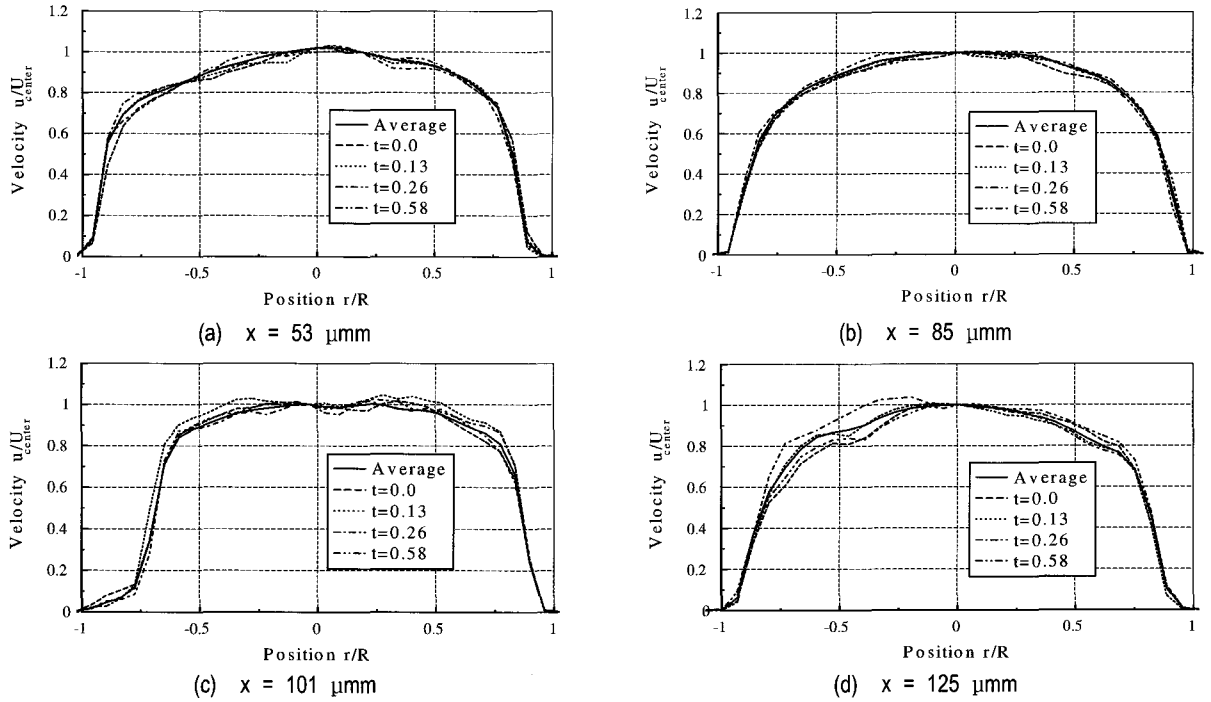

Figure 6 Ensemble-averaged axial velocity profiles normalized using vessel diameters and velocities at the center in four cross sections.

μm in Fig. 5 (d) shows asymmetric, particularly. A very low velocity region at (c) x = 101 μm was identified near the downside wall due to a marginal cell-free plasma layer. The profile at (c) x = 101 μm in particular shows the typical flow features for a non-Newtonian fluid; a more broad axial velocity distribution and a steep velocity gradient near the wall. At x = 125 μm in Fig. 5 (d), for the smallest diameter section, the dip was not observed and the cell-free plasma layer was less predominant. The maximum velocity of downside at x = 125 μm in Fig. 5 (d) showed larger. It is considered that the vessel wall in downside around x = 110 μm curved to upper resulting in reducing the vessel diameter. Figure 6 shows normalized axial blood velocity profiles in four sections using vessel radiuses R and the axial velocities at the center of each time in three cross sections. The velocity distributions

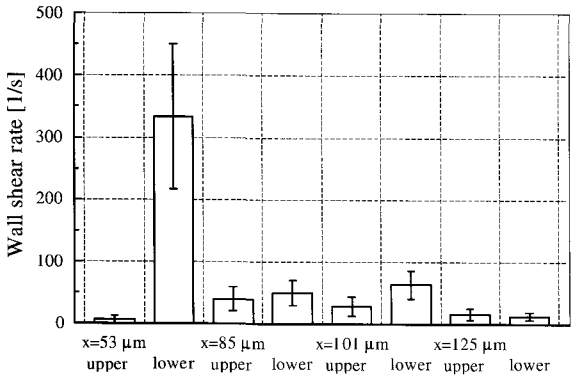

Figure 7 Time-averaged wall shear rates at the upper and lower wall in four cross sections. (The values are expressed in mean and SD).

at x = 85 μm in Figure 6 (b) have nearly the same profile. Very low velocity regions near both sides of wall were slightly observed in a plasma layers. That region near left side of wall at x = 101 μm in Figure 6 (c) spread widely. The profile around center became flat and hollow. The profile in the left side at x = 125 μm in Figure 6 (d) had larger fluctuation.

A wall shear rate (WSR) is widely used to assess adhesion of cells, influence toward endothelium structure and metabolism of arterial wall and so on. However, since it is difficult to measure WSR directly in a small vessel, WSR was calculated by analogy to that of a Newtonian fluid under conditions of Poiseuille flow, i.e., WSR = $8V_{mean}$ / D. Here, V_{mean} and D represent mean velocity and vessel diameter. In the present study, velocity distributions with high spatial resolution even close to vessel walls were obtained. Figure 7 shows time-average wall shear rates and variances in four cross-sections, calculated using axial velocity profiles numerically. All of WSRs except for lower wall at x = 53 μm were rather smaller than them of Poiseuille flow. Large difference between WSRs of upper and lower walls at x = 101 μm was observed because of difference of thickness of plasma layer. WSR of lower wall at x = 53 μm was largest about 300 s^{-1}, because plasma layer was very thin due to centrifugal force caused by curvature of vessel.

Discussion and Conclusion

A number of studies have obtained velocity profile in vivo using various imaging techniques[8-11,19], in which velocity vectors have been determined by tracing visualized individual cells or clustering cells. The imaging technique has potential to measure a velocity distribution in microvessels. However, the previous studies have not shown enough spatial resolution and good accuracy in velocity measurement. There are two ways to improve these. One is to improve hardware, mainly optics and camera, and the other is to improve the software for image analysis. In the field of experimental fluid dynamics, particularly in turbulence, image analysis technique such as PIV method has been rapidly progressed to overcome that problem. The authors have developed a highly PIV technique to complete highly accurate and wide-dynamic-range measurements[16]. This technique, which consists of cross- correlation method and gradient sub-pixel analysis method, has potential for producing fine velocity profiles even very close to vessel wall.

Blood velocity profiles in microvessels became more blunt as the velocity decreased and cells aggregated[19,20]. As shown in Figures 5 and 6, the velocity profiles at x = 85 and 101 μm with smallest velocities became blunt, and profile at x = 125 μm with largest velocity become sharp. The profile at x = 101 μm with thick plasma layer are most blunt.

In the present study, the WSR wall was significantly small, compared with those in the Poiseuille flow. Moreover, large difference in the WSR appeared at several cross-sections (Figure 7). In general, the wall stress in microvessels varies according to the height, orientation and slenderness of the cells[21,22] Recent studies have shown that the microvascular endothelium is covered with an endothelial surface layer (ESL) with 0.5^{-1} μm thickness[23,24]. Pries et al [25] showed that flow resistance in microvessels were substantially higher than that in glass tubes with corresponding diameters. The reason was considered of be influenced by the existence of ESL[26]. The WSR might be influenced by the existence of ESL.

In summary, micro PIV technique, which consists of the intravital-microscope and high-speed digital video system, was applied to in vivo blood images

of an arteriole in a rat mesentery. The velocity distributions with spatial resolutions of 0.8 × 0.8 μm were measured even near the wall in the center plane of arteriole. By making ensemble-averaged time-series of velocity distributions, velocity profiles over different cross-sections were calculated for comparison. The shear rate at the vascular wall also evaluated on the basis of the ensemble-averaged profiles. It was shown that the velocity profiles were blunt in the center region of the vessel cross-section while they were steep in the near wall region. The wall shear rates were significantly small, compared with those estimated from the Poiseuille profiles.

References

1. Oka S. Cardiovascular Hemorheology, Cambridge University Press, 1981; Chap 3, Chap.5.
2. Wayland H and Johnson PC. Erythrocyte velocity measurement in microvessels by two-slit photometric method. J. Appl. Physiol. 1967;22:333-337.
3. Intaglietta M, Silverman NR and Tompkins WR. Capillary flow velocity measurements in vivo and in situ by television methods. Microvasc. Res. 1975;10:165-179.
4. Sato M, and Ohshima N. Velocity profiles of blood flow in microvessels measured by ten channels' dual-sensor method. Biorheology. 1988;25:279-288.
5. Yamaguchi S, Yamakawa T, and Niimi H. Cell-free plasma layer in cerebral microvessels, Biorheology 1992;29:251-260.
6. Cochrane T, Earnshaw J C, Love AHG. Laser Doppler measurement of blood velocity in microvessels. Med Biod Eng Comput. 1981; 19:589-596.
7. Seki J, Sasaki Y, Oyama T and Yamamoto J. Fiber-optic laser-Doppler anemometer microscope applied to the cerebral microcirculation in rats. Biorheology 1996;33:463-470.
8. Tangelder GJ, Slaaf DW, Muijtjens AMM, Arts T. Oude Egbrink MGA and Reneman RS. Velocity profiles of blood platelets and red blood cells flowing in arterioles of the rabbit mesentery. Circ. Res. 1986;59:505-514.
9. Tangelder GJ, Slaaf DW, Arts T and Reneman RS. Wall shear rate in arterioles in vivo: least estimates from platelet velocity profiles. Am. J. Physiol. 1988;254:H1059-H1064.
10. Parthasarahi AA, Japee SA and Pittman RN. Determination of red blood cell velocity by shuttering and image analysis. Ann. Biomed. Eng. 1999;27:313-325.
11. Tsukada K, Minamitani H, Sekizuka E and Oshio C. Image correlation method for measuring blood flow velocity in microcirculation: correlation 'window' simulation and in vivo image analysis. Physiol. Meas. 2000;21:459-471.
12. Reike W, Jonhson PC, Gaehhtgens P. Effect of shear rate variation on apparent viscosity on human blood in tubes of 29 to 94 um diameter, Circ Res. 1986;59:124-132.
13. Yamaguchi S, Yamakawa T and Niimi H. Red cell velocity and microvessel diameter measurement by a two fluorescent tracer method under epifluorescence microscopy: Application to cerebral microvessels of cats. Int. J. Microcirc. 1992;11:403-416.
14. Keane RD and Adrian RJ. Theory of cross-correlation analysis of PIV. Applied Scientific Research. 1992;49:191-215.
15. Raffel M, Willert CE and Kompenhans J. Particle image velocimetry. Springer 1998.
16. Sugii Y, Nishio S, Okuno T and Okamoto K. A highly accurate iterative PIV technique using gradient method. Meas. Sci. Technol. 2000;11:1666-1673.
17. Nakano A, Sugii Y, Minamiyama M, Niimi H. Measurement of red cell velocity profile and wall shear-rate at arteriolar bifurcation using high speed videomicroscopic particle image velocimetry, Microcirculation annual 2002;18: 125-126.
18. Sugii Y, Nishio S and Okamoto K. In Vivo PIV Measurement of Red Blood Cell Velocity Field in Microvessels Considering Mesentery Motion. Physiol. Meas. 2002;23:403-416.

19. Bishop JJ, Nance PR, Popel AS, Intaglietta M, Johnson PC. Effect of erythrocyte aggregation on velocity profiles in venules. Am J Physiol Heart Circ Physiol 2001;280:H222-H236.
20. Schmid-Schonbein GW and Zweifach BW, RBC velocity profiles in arterioles and venules of the rabbit omentum. Microvasc Res. 1975; 10:153-164.
21. Satcher Jr RL, Bussolari SR, Gimbrone Jr MA and Dewey Jr CF. The distribution of fluid forces on model arterial endothelium using computational fluid dynamics. J. Biomech. Eng. 1992;114:309-316.
22. Barbee KA, Mundel T, Lal R and Davies PF, Subcellular distribution of shear stress at the surface of flow-aligned and nonaligned endothelial monolayers. Am. J. Physiol. 1995; 268:H1765-H1772.
23. Desjardins C. and Duling BR. Heparinase treatment suggests a role for the endothelial cell glycocalyx in regulation of capillary hematocrit. Am. J. Physiol Heart Circ Physiol 1990;258:H647-H654.
24. Vink H and Duling BR, Identification of distinct luminal domains for macromolecules, erythrocytes and leukocytes within mammalian capillaries, Circ Res 1996;79:581-589.
25. Pries AR, Secomb TW, Gessner T, Sperandio M B, GrossJ F and Gaehtgens P. Resistance to blood flow in microvessels in vivo. Circ Res 1994;75:904-915.
26. Pries AR, Secomb TW, Jacobs H, Sperandio M, Osterloh K and Gaehtgens P. Microvascular blood flow resistance: role of the endothelial surface layer. Am. J. Physiol Heart Circ. Physiol. 1997;273:H2272-H2279.